Earth Reinforcement, Ochiai, Yasufuku & Omine (eds) © 1996 Balkema, Rotterdam. ISBN 90 5410 833 9

Limit design of earth reinforcement methods considering displacement field

K.Arai
Fukui University, Japan

K.Kasahara
Maeda Kosen Co., Ltd, Fukui, Japan

ABSTRACT: This paper proposes a limit design technique for slope and retaining wall reinforced by geotextile, which is tentatively called LSFEA (Limit State Finite Element Analysis). LSFEA, which is fundamentally based on the initial stress method for nonlinear stress-strain analysis in FEM, aims to fill a large gap existing between FEM and LEM (Limit Equilibrium Method) which is a traditional design technique also in earth reinforcement problems. LSFEA employs Mohr-Coulomb and Coulomb yield criteria respectively for soil mass and friction interface. By assuming a linear elastic response before yielding and a non-associated flow rule after yielding as a stress-strain relationship, LSFEA provides a definite collapse mode similar to a potential slip surface assumed in LEM. It is difficult for LEM to consider the kinematical condition at failure and the stiffness of material. LSFEA enables to compensate for most of these defects in LEM, because LSFEA is based on FEM. LSFEA can be effectively applied to stability problems in which the kinematical condition and material stiffness largely affect the solution.

1 SUMMARY OF LSFEA

LSFEA should be regarded as a modified initial stress method for nonlinear stress-strain analysis which was originally developed by Zienkiewicz et al. (1969). LSFEA applies the initial stress method at only one loading stage as illustrated later in Fig. 3, by assuming both linear elastic response before yielding and the non-associated flow rule after yielding. As the result, LSFEA changes the distribution of yield finite element in the iteration cycle for the initial stress method. These two operations seem important for finding a reasonable failure region of the stability problem.

Yield Criterion: : Mohr-Coulomb and Coulomb yield criteria are employed respectively to soil mass and the friction interface between structure and soil.

Mohr-Coulomb: $F_M=$
$\{(\sigma_x-\sigma_y)^2+4\tau_{xy}^2\}^{1/2}-\{(\sigma_x+\sigma_y)\sin\phi+2c\cos\phi\}=0$
Coulomb:
$F_C=|\tau|-c-\sigma_n\tan\phi=0$ (1)

where σ_x, σ_y and τ_{xy}: stress components, σ_n: normal stress, τ : shear stress, and c and ϕ: strength parameters. For the friction interface we employ the thin layer finite element proposed by Desai et al. (1984).

Stress-Strain Relationship : Both for Mohr-Coulomb and Coulomb materials, a linear elastic response is assumed before yielding. Subjected to Coulomb material, Fig. 1 schematically illustrates the relationship between stress vector $\{\sigma\}$ and strain vector $\{\varepsilon\}$. Point B in Fig. 1 corresponds to a final equilibrium state at an arbitrary position within a failure region. Considering the stress history, it seems reasonable to assume that the stress trajectory firstly attains to the yield surface not at the final state B but at another point A in Fig. 1. As seen in Fig. 1, after reaching the yield surface at point A, it is assumed that the stress path moves along the yield surface, and that the movement along the surface is purely plastic. At the plastic state, we employ the non-associated flow rule and a plastic potential

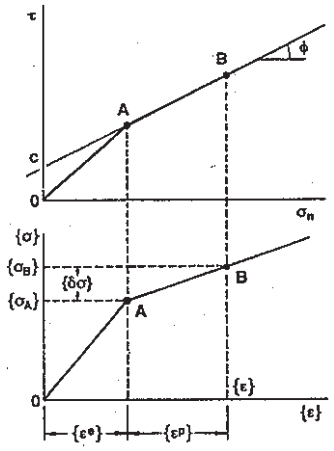

Fig. 1. Stress-strain relationship (Coulomb material)

defined by Fig. 2 and the following equations (see Mroz, 1980).

Mohr-Coulomb: Q_M=
$\{(\sigma_x-\sigma_y)^2+4\tau_{xy}^2\}^{1/2}-\{(\sigma_x+\sigma_y)\sin\nu+2g\cos\nu\}=0$
Coulomb
$Q_C=|\tau|-g=0$ (2)

where g: a hypothetical parameter which is not cited actually, because Eq. (2) is used only by its differential form, and ν: dilatancy angle (see Fig. 2a) which is considered to be zero in this paper. By using the yield criterion and plastic potential, the stress-strain relatinship at plastic state is given as

$$\{\delta\sigma\}=[D^{ep}]\{\varepsilon^p\} \quad (3)$$

where $\{\delta\sigma\}$:stress increment at plastic state, $\{\varepsilon^p\}$:plastic strain (see Fig. 1), and $[D^{ep}]$: stress-strain matrix at plastic state which is calculated by as well known formula (see Zienkiewicz et al. 1969). Both soil mass or Mohr-Coulomb material and friction interface are assumed not to bear tensile stress.

$$\text{Mohr-Coulomb: } \sigma_3\geq 0,\ \text{Coulomb: } \sigma_n\geq 0 \quad (4)$$

Numerical Procedure : Since we are concerned with only the final equilibrium state of soil-structure, the initial stress method is applied at only one loading stage as shown in Fig. 3, where initial stress $\{\sigma_0\}$ and elastic stress $\{\sigma_E\}$ are defined. Such an application of the initial stress method makes it necessary to modify a part of method. Fig. 4 shows the flow chart of numerical procedure, where $\{u\}$: nodal displacement, $[K]$: stiffness matrix, $\{f\}$: total load vector, $[B]$; matrix for calculating strain components from $\{u\}$, and V : volume of the element. Referring to Figs. 3 and 4, we must decide simultaneously two kinds of stresses, yield stress $\{\sigma_A\}$ and initial stress $\{\sigma_0\}$. $\{\sigma_0\}$ is determined so as to satisfy the iteration loop shown in Fig. 4, while $\{\sigma_A\}$ has to be isolated by an appropriate assumption because we do not necessarily follow the loading history but are concerned with only the final equilibrium state. Arai (1993) tried to isolate $\{\sigma_A\}$ so as to minimize the total plastic work until the final state. The minimization of total plastic work requires a lot of computational effort, and $\{\sigma_A\}$ must be determined many times in the iteration step as stated later. Thus in this paper we employ the following simpler and more practical method which was proposed Zienkiewicz et al. (1969). As shown in Fig. 3, $\{\sigma_I\}$ denotes an actually initial state of stresses. Referring to Fig. 3, assume as

$$\{\sigma_A\}=\{\sigma_I\}+r(\{\sigma_E\}-\{\sigma_I\}) \quad (5)$$

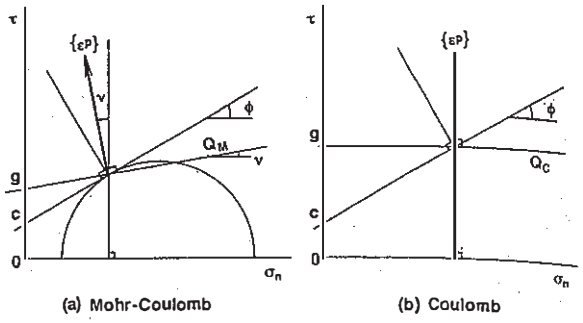

Fig. 2. Non-associated flow rule

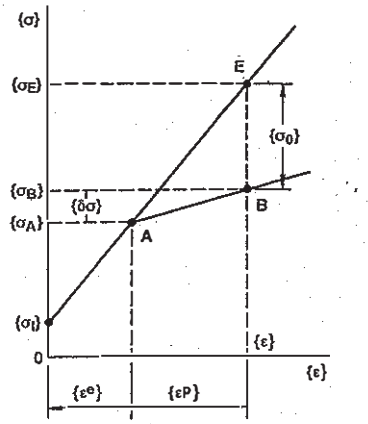

Fig. 3. Initial stress method

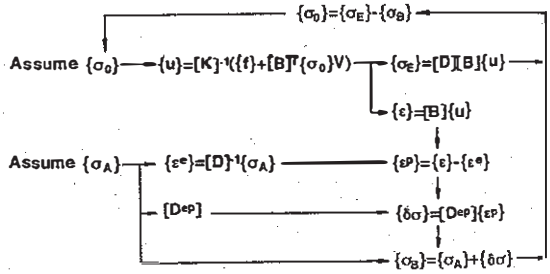

Fig. 4. Numerical procedure

By linear interpolation, r is found for Coulomb material as

$$r=-F_C(\{\sigma_I\})/[F_C(\{\sigma_E\}-F_C(\{\sigma_I\})] \quad (6)$$

When applying this method to Mohr-Coulomb material, due to nonlinearity in the yield function, we must employ a better estimate of r proposed by Nayak et al. (1972)

Iteration Scheme : Stage1: Assume the trial values of initial stress $\{\sigma_0\}$ to be zero. Stage 2: Determine $\{\sigma_0\}$ and $\{\sigma_A\}$ by the following steps. 2a) Applying both total load vector $\{f\}$ and correction load vector

$\{f_0\}=[B]^T\{\sigma_0\}V$, solve the elastic problem. 2b) Find the yield finite elements which attain to the state of plastic equilibrium. 2c) For the yield finite elements, determine yield stress $\{\sigma_A\}$ by Eqs. (5) and (6). Once $\{\sigma_A\}$ is decided for each yield element, the value is stored and used throughout Stage 2. 2d) Calculate final stress $\{\sigma_B\}$ in Fig. 2, using $\{\sigma_A\}$ found at step 2c). And modify initial stress $\{\sigma_0\}=\{\sigma_E\}-\{\sigma_B\}$. 2e) Repeat steps 2a) to 2d) until convergence is obtained. Stage 3: Repeat Stage 2 several times, by replacing the initial stresses at the first cycle with those obtained at the preceding stage, until the change in $\{\sigma_B\}$ reaches a sufficiently small value. Stage 3 is required because both the yield finite elements and the initial stresses decided at Stage 2, are those corresponding to a particular yield stress $\{\sigma_A\}$ which was determined against the initially assumed values of initial stresses. The constraints given by Eq. (6) is satisfied easily by the initial stress method (see Zienkiewicz et al. 1968).

2 APPLICATIONS

2.1 Example 1

The first example (see Fig. 5) considers the effect of reinforcement in slope stability problem. In all the following case studies, actual initial stresses in soil stratum $\{\sigma_I\}$ are supposed negligibly small. The material parameters are also given in Fig. 5, where E: Young's modulus, μ: Poisson's ratio, γ: unit weight, and A: area of cross section of geotextile. The geotextile is represented by a conventional truss element, and is assumed to bear no compressive force. Fig. 6 shows the failure region or the distribution of yield finite element provided by LSFEA when changing safety factor of shear strength F_S, which is defined as

$$F_S=c_m / c=\tan\phi_m / \tan\phi \qquad (7)$$

where c, ϕ: actual strength parameters introduced previously, and c_m, ϕ_m: current and provisional strength parameters. Since the calculation of F_S requires to suppose such a hypothetical condition, some combinations of F_S and the values of strength parameters happen to produce an unreasonable collapse mode different from the actual mode likely to exist. In Fig. 6, note that the succeeding result for each F_S is found by regarding each state as a final equilibrium state, and the result is independent of the preceding state for smaller F_S. Fig. 6 shows also the tensile region at which Eq. (4) is satisfied only by using the initial stress method. When applying LSFEA to a slope stability problem, we increase the value of F_S step by step as seen in Fig. 6. We decide the critical value of F_S by using the first

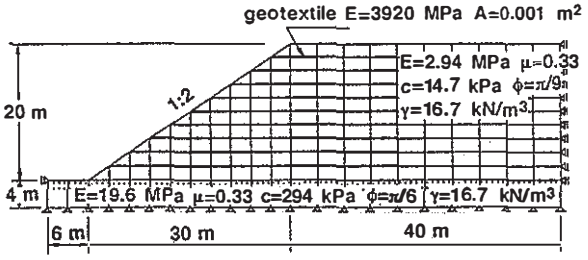

Fig. 5. Finite element model in Example 1

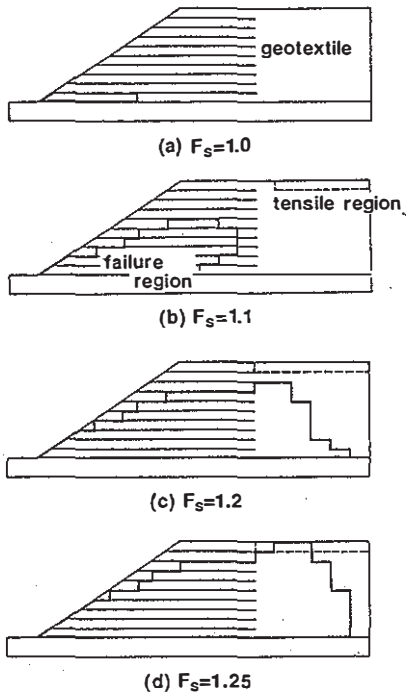

Fig. 6. Failure region (reinforcement)

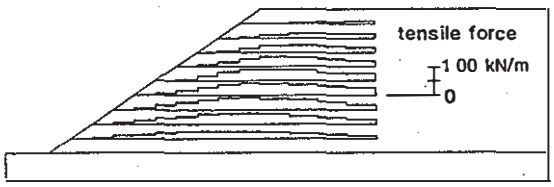

Fig. 7. Tensile force distribution on geotextile

occurrence of a global collapse mode. The global collapse mode herein means that the yield finite elements distribute continuously from the toe to the top of slope as seen in Fig. 6(d). Being different from the assumption employed in traditional design scheme, at the collapse state the reinforcement method tends to enlarge considerably the failure region outside of reinforced area. However it should be repeatedly emphasized that the failure

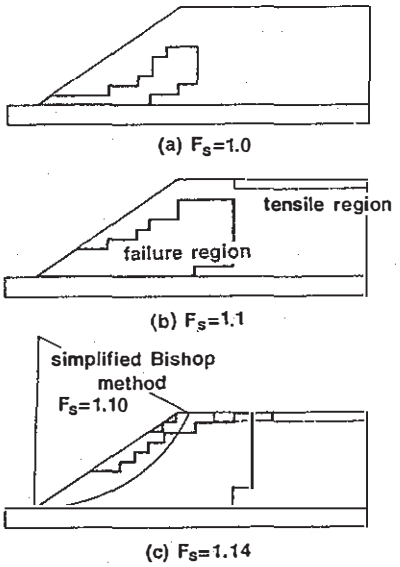

Fig. 8. Failure region (no reinforcement)

region shown in Fig. 6(d) is created for the hypothetical strength parameters reduced by F_S. Fig. 7 illustrates the distribution of tensile force acting on reinforcement material at the final state. Fig. 8 shows the failure and tensile regions when no reinforcement is employed. Fig. 8(c) shows also the critical slip surface and the safety factor given by the simplified Bishop method in which a slip surface is assumed to be circular. LSFEA and the simplified Bishop method provide a close value of safety factor, while these two methods create a little different failure region. Comparing Fig. 6 with Fig. 8, the earth reinforcement in this particular case, appears to increase the safety factor from 1.1 to 1.25. Conventional design concept for earth reinforcement method which is based on LEM, tends to evaluate a reinforcement material only by its final strength, and to neglect its stiffness which restricts the deformation of soil mass and which may largely contribute to the improvement of slope stability. LSFEA enables to discuss the plastic equilibrium state and collapse mechanism, considering the stiffness of material and the displacement field of geotechnical structure.

2.2 Example 2

The second example (see Fig. 9) considers the lateral earth pressure problem where two sheets of truss material are spread within the homogeneous backfill and connected to the rigid retaining wall. The values of material constants are given in Table 1. The reinforcement material is represented by the assemblage of truss elements and supposed to bear compressive force only in this particular example. The stiffness of reinforcement material is 3.92 MN/m. Fig. 10(a) illustrates the results calculated by LSFEA when no reinforcement is employed. Fig. 10(b) shows the results by LSFEA when the

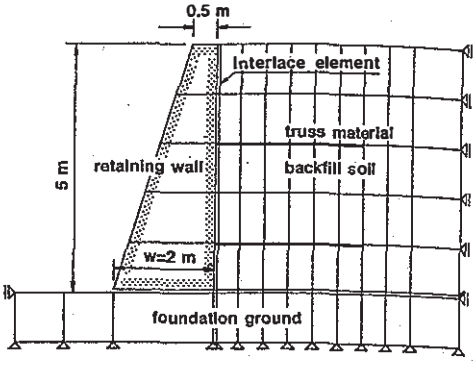

Fig. 9. Finite element model in Example 2

Table 1. Material Constants in Example 2

	E MPa	μ	G_i MPa	c kPa	ϕ deg.	ν deg.	γ kN/m³
retaining wall (concrete)	5880	0.16	—	490	45	0	21.6
backfill soil	4.9	0.3	—	0	30	0	15.7
foundation ground	9.8	0.3	—	49	30	0	0
interface between wall and backfill	4.9	0.3	4.9	0	20	—	—
interface between wall and foundation	9.8	0.3	4.9	0	20	—	—

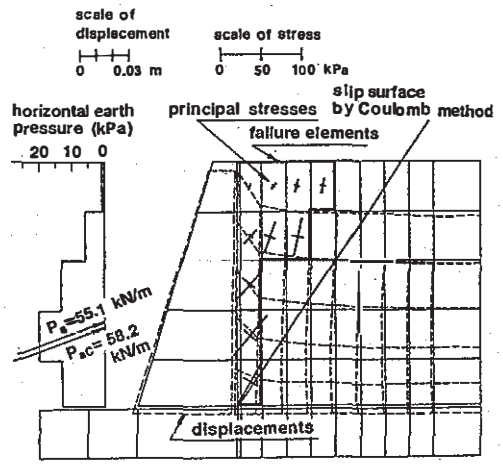

(a) No reinforcement

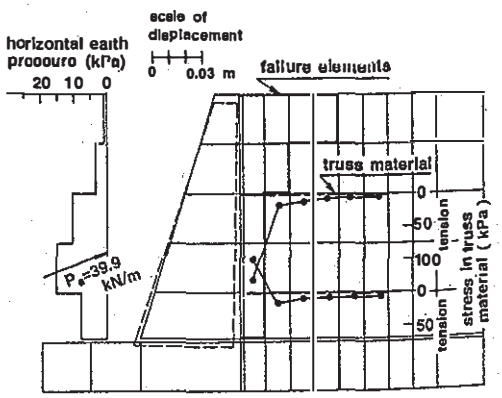

(b) Reinforcement

Fig. 10. Result in Example 2

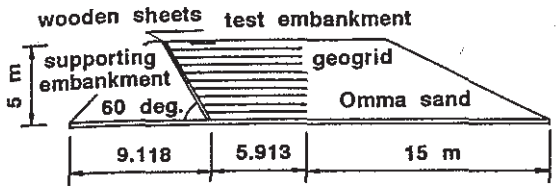

Fig. 11. Field test

reinforcement shown in Fig. 9 is applyed. In Fig. 10, the broken line represents the displacements of wall and backfill, P_a: active thrust by LSFEA, and P_{aC}: active thrust given by Coulomb method in which a triangular distribution of earth pressure is assumed. The truss material reduces about 27% of the active thrust. Note that irrespective of earth reinforcement, both the failure region and wall movements are almost the same as seen in Figs. 10 (a) and 10(b).

2.3 Example 3

The third example (see Fig. 11) studies a test embankment reinforced by geogrids and non-woven geotextiles, which was actually constructed in Kanazawa, Japan. Fig. 11 illustrates the longitudinal cross section of field test. When the supporting embankment shown in Fig. 11 is removed, the test embankment has an overhanging slope at angle of 60 deg. to the ground surface. The detailed explanation of construction procedure, observed performance and so on are reported by Goren et al. (1984). The test embankment was carried out twice at the same place. The first test employed a strong and highly stiff geogrid, and the overhanging embankment was stable. The second test used a weak and less stiff material, and the test embankment had failed before the supporting embankment in Fig. 11 was removed completely. Fig. 12 shows the finite element meshing and material constants employed. The results calculated by LSFEA are given in Figs. 13 and 14. Especially the deformation behavior illustrated in Fig. 14 may agree fairly well with the observed results in the field test. It is interesting to note that the failure region spreads considerably within the embankment as seen in Fig. 13(a), whereas the deformation of embankment appears small.

3 CONCLUSIONS

The results of case studies prove that LSFEA provides a physically reasonable solution of earth reinforcement problem. LSFEA does not intend to simulate soil behavior but does to be applied to the practical limit design based on stability analysis. It is important to emphasize that LSFEA produce a

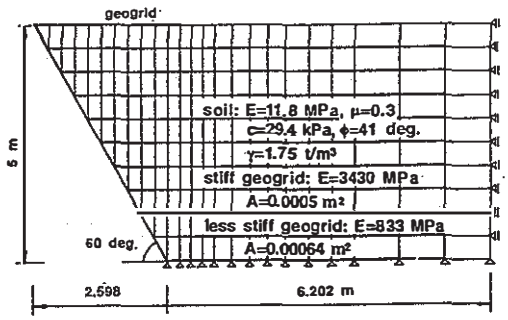

Fig. 12. Finite element meshing in Example 3

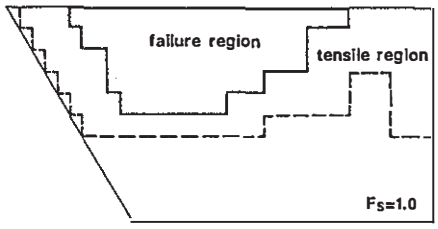

(a) Stiff geogrid

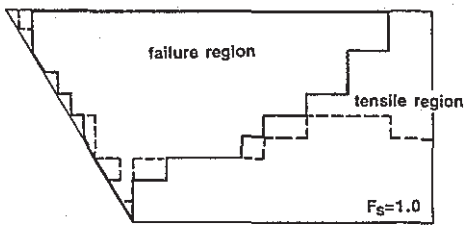

(b) Less stiff geogrid

Fig. 13. Failure region

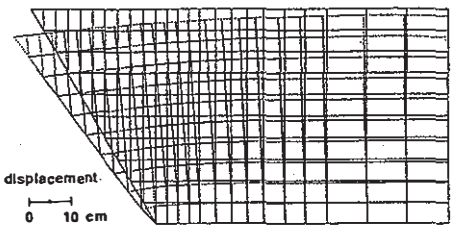

(a) Stiff geogrid

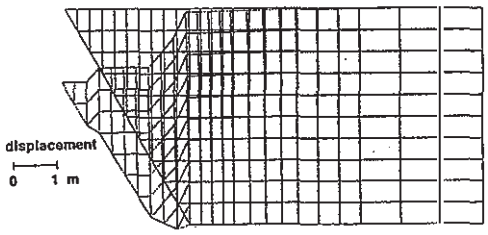

(b) Less stiff geogrid

Fig. 14. Distribution of displacement

definite collapse mechanism similar to the potential slip surface assumed in LEM, and that the collapse mechanism is supported by a kinematically admissible displacement field, statically admissible stress field, and a suitable stress-strain relationship.

REFERENCES

Arai, K. 1993. Active earth pressure founded on displacement field. Soils and Foundations. 33-3: 54-67.

Desai, C.S., Zaman, M. M., Lightner, J. G. and Siriwardane, H. J. 1984. Thin-layer element for interface and joints. Int. J. Numer. Anal. Methods Geomech. 8: 19-43.

Goren, S., Ohta, H., Yamakami, T., Morikage, A. and Yokota, Y. 1994. Performance of test embankment reinforced by geosynthetics. 29th Japan National Conf. SMFE, 25-28.

Mroz, Z. 1980. Deformation and flow of granular materials. Mechanics of Solids. 119-132.

Nayak, G.C., and Zienkiewicz, O. C. 1972. Elasto-plastic stress analysis. Int. J. Numer. Methods Eng. 5: 113-135.

Zienkiewicz, O.C., Valliappan, S. and King, I. P. 1968. Stress analysis of rock as a 'no tension' material. Geotechnique. 18: 56-66.

Zienkiewicz, O.C., Valliappan, S. and King, I. P. 1969. Elastoplastic solutions of engineering problems 'initial stress' finite element approach. Int. J. Numer. Methods Eng. 1: 75-100.